Cluster model studies on oxygen sites at the (010) surfaces of V$_2$O$_5$ and MoO$_3$

K. Hermann [a,*], A. Michalak [b], M. Witko [c]

[a] *Fritz-Haber-Institut der MPG, Faradayweg 4–6, D-14195 Berlin, Germany*
[b] *Department of Computational Methods in Chemistry, Faculty of Chemistry, Jagiellonian University, R. Ingardena 3, 30060 Cracow, Poland*
[c] *Institute of Catalysis and Surface Chemistry, Polish Academy of Sciences, ul. Niezapominajek, 30239 Cracow, Poland*

Abstract

Cluster model studies have been performed to examine the electronic structure and adsorption properties near structurally different oxygen sites at the (010) surfaces of vanadium pentoxide, V$_2$O$_5$, and molybdenum trioxide, MoO$_3$. In addition, adsorption of hydrogen at the oxygen sites and desorption of OH groups has been studied in order to find site specific differences. The electronic properties and total energies of the clusters have been obtained from ab initio density functional theory (DFT) calculations. The surface oxygen sites are found to be ionic where bridging oxygens become more negative than terminal ones. Further, hydrogen adsorbs at all oxygen sites where binding is strongest at the bridge sites on the V$_2$O$_5$(010) surface whereas on MoO$_3$(010) the terminal sites are preferred. The latter difference can be understood by simple geometric arguments. Surface OH groups formed by H adsorption and involving terminal oxygens are strongly bound to the surface whereas those involving bridging oxygens are mobile and become available for subsequent reactions.

Keywords: Density functional theory; Cluster calculations; Oxidation; Adsorption; Molybdenum oxide; Vanadium oxide

1. Introduction

Transition metal oxides are characterized by a wealth of interesting physical and chemical properties which explains their use as materials in chemical and electronic industries [1,2]. These materials exist in many crystallographic forms with stoichiometries differing only slightly from each other and transition metal ions exhibiting various oxidation states. Their specific catalytic properties follow from the ability to easily undergo surface oxidation and reduction combined

with usually high densities of cationic and anionic vacancies. Surface cations and anions can form (Lewis) acid and base sites as well as acid–base pair sites which influence the electronic structure and affect respective surface properties.

Vanadium and molybdenum oxides are of great scientific importance since their chemical behavior is very complex. These oxides, prepared as pure substrates or as compounds including other transition metals, are found to act as catalysts in many reactions of rather different type [2]. In particular, vanadium pentoxide, V$_2$O$_5$, and molybdenum trioxide, MoO$_3$, based materials play an important role as catalysts in

---

* Corresponding author.

the selective oxidation of hydrocarbons [3,4]. Here the catalyst surface performs a complex multi-step operation on the reacting molecule by activating some of the bonds within the reactant and hindering interactions which could result in unwanted products. In a first step hydrocarbon molecules are activated by hydrogen abstraction near specific surface oxygen sites which leads to formation of surface OH groups. Subsequently, surface OH can react with hydrocarbons which results in nucleophilic insertion of oxygen forming acid type products. Here it is important to know which of the structurally different surface oxygen sites is involved in the different steps of the oxidation reaction.

In the present study we examine the electronic structure and bonding properties of geometrically inequivalent surface oxygen sites at the (010) surfaces of ideal V_2O_5 and MoO_3. In addition, we study adsorption of hydrogen at these oxygen sites and desorption of OH groups in order to find site specific differences. The local surface environment about the oxygens is represented by bond saturated clusters [5,6] as described below. Electronic wavefunctions and respective properties such as local charging or bond saturation are determined by ab initio density functional theory (DFT) calculations based on linear combinations of Gaussian type atomic orbitals. Population analyses confirm the ionic nature of both oxides as suggested by basic chemical intuition. The surface oxygen sites are found to be always partly ionic where oxygens O(b,c) bridging between surface metal centers become more negative than terminal (vanadyl/molybdenyl) oxygens O(a) coordinated to one metal center. The increased charging at the bridging oxygen sites hints at their increased local reactivity with respect to nucleophilic attacks.

Total energy calculations for hydrogen approaching the clusters at different surface oxygen sites yield strong adsorptive binding at all sites with appreciable ionic contributions. The latter is confirmed by the result that on both substrates the oxygen sites which lead to

strongest O–H binding coincide with those where the electrostatic potentials of the cluster charge distributions assume their (negative) minima: open bridging oxygen sites, O(c), on V_2O_5 (010) and terminal oxygen O(a) sites on MoO_3 (010). Further, total energy curves for desorption of surface OH formed by H adsorption at the different oxygen sites show that OH groups involving terminal oxygens are strongly bound to the surface. In contrast, binding curves for hydroxyls involving bridging oxygens are always rather shallow near the H adsorption geometry which suggests that these OH groups are quite mobile and become available for subsequent reactions.

2. Computational details

Vanadium pentoxide, V_2O_5, is described by a layer type orthorhombic crystal structure [3] where the layers lie parallel to the (010) netplane representing the easy cleavage plane of the crystal, see Fig. 1a. The layers are characterized by a periodic arrangement of edge and
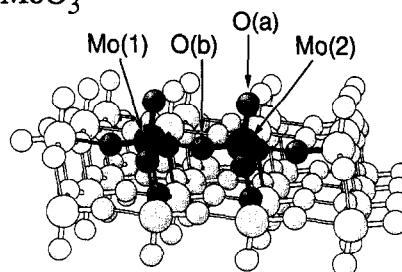
a) V_2O_5
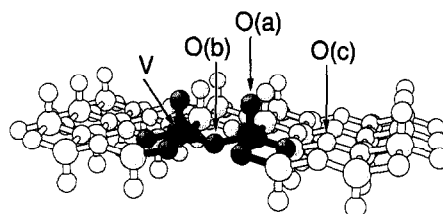
b) MoO_3

Fig. 1. Representative (010) (bi)layers of the ideal V_2O_5 (Fig. 1a) and MoO_3 (Fig. 1b) crystal lattices where the different oxygen sites are labeled accordingly. The clusters used in the present study are shown by darker balls.

corner sharing VO_5 pyramids sticking out at both sides of the layers. As a consequence, the ideal (010) surface of V_2O_5 contains three structurally different surface oxygens, the terminal (vanadyl) oxygens O(a) coordinated to one vanadium atom, the oxygens O(b) bridging two vanadyl groups, and the oxygens O(c) bridging two bare vanadium centers where the O(b,c) centers can be coordinated to two or three vanadium atoms. Molybdenum trioxide, MoO_3, forms also a layer type orthorhombic crystal structure [4] where bilayers lie parallel to the (010) netplane, see Fig. 1b. The bilayers can be characterized by two sublayers consisting of a periodic arrangement of distorted MoO_6 octahedra where oxygen ions are shared between adjacent octahedra within and between the sublayers. While the internal interaction between atoms of the bilayers is determined by rather strong ionic and covalent bonding adjacent bilayers couple via weak Van der Waals forces. The ideal MoO_3 (010) surface contains three structurally different surface oxygens. The terminal (molybdenyl) oxygens O(a) are coordinated to one molybdenum atom, the oxygens O(b) bridging two molybdenyl groups asymmetrically are coordinated dominantly to one molybdenum atom, and the oxygens O(b') bridging two molybdenyl groups symmetrically are coordinated to three molybdenum atoms. (Results for symmetrically bridging oxygens will be discussed elsewhere [7].)

The above mentioned oxygen surface sites are indicated in Fig. 1 for both crystals. Their geometric environment determines the shape of local model clusters considered in this study. The smallest cluster describing all V_2O_5 (010) oxygen sites meaningfully is V_2O_9, see Fig. 1a. This cluster is used in the present calculations where peripheral oxygens are electronically saturated by hydrogen atoms yielding $V_2O_9H_8$. The additional hydrogens, simulating cluster embedding, are placed such that the bond order of each peripheral oxygen in its ideal bulk environment is obtained. Thus, four equivalent bottom oxygens (at the short cluster side) bind

one hydrogen each and two bottom oxygens (at the long cluster side) bind two hydrogens. The smallest meaningful cluster representing the MoO_3 (010) oxygen sites is Mo_2O_{11}, see Fig. 1b. This cluster is also augmented by additional hydrogen atoms to saturate peripheral oxygen bonds following the above bond order scheme which results in $Mo_2O_{11}H_{10}$. While the present communication focuses on results from the two small clusters indicated in Fig. 1 it should be noted that more recent studies based on much larger surface clusters for both materials [7] confirm all qualitative conclusions drawn from the present calculations.

Electronic wavefunctions and derived properties of the clusters are determined within the framework of ab initio density functional theory (DFT) [8] where Kohn–Sham orbitals are represented by linear combinations of atomic orbitals (LCAOs) using extended basis sets of contracted Gaussian-type orbitals (CGTO's). The bases were taken from DFT optimizations [9] and were all-electron type for all V, O, and H centers while the Mo centers were represented by smaller valence bases with the $[Ar]3d^{10}$ cores described by model core potentials [10]. For the calculations the program package DeMon [11] was applied using the local spin density approximation (LSDA) for exchange and correlation based on the Vosko–Wilk–Nusair functional [12]. The electronic structure of the clusters is analyzed by Mulliken population analyses [13], bond order indices [14], electron charge densities, and electrostatic potential distributions [15].

While the pure substrate clusters $V_2O_9H_8$ and $Mo_2O_{11}H_{10}$ are treated as electronically neutral (closed shell) systems the interaction curves for H adsorption and OH desorption are calculated for the respective positively charged clusters $(V_2O_9H_8H)^+$ and $(Mo_2O_{11}H_{10}H)^+$. This procedure decreases the computational effort without loss of accuracy since the lowest unoccupied orbitals (LUMO) of the cluster ions are located at the cluster periphery and do not take part in the H adsorption, OH desorption as discussed elsewhere [17].

3. Results and discussion

Table 1 lists calculated populations and bond orders obtained from the $V_2O_9H_8$ cluster representing the V_2O_5 (010) surface and from $Mo_2O_{11}H_{10}$ representing MoO_3 (010). Here the quantitative data should be taken with care due to principal limitations in the analysis methods whereas the qualitative findings of Table 1 are meaningful. While the vanadium centers are described by positive ions $V^{+1.0}$ both oxygens form negative ions ($O^{-0.3}$ for the terminal and $O^{-0.5}$ for the bridging oxygens, see Table 1a) which is expected from chemical intuition. Further, as a result of the metal coordination bridging oxygen centers carry more negative charge than terminal ones. In addition to ionic binding between the charged atom centers at the surface there are covalent contributions which are reflected in the bond order results. The O–V bonds involving terminal oxygens O(a) are described by bond orders near 2 suggesting O = V double bonds which is consistent with their coordination scheme. On the other hand, O–V bonds involving bridging oxygens O(b,c) result in bond orders near 1 and thus O–V single

bonds in accordance to their coordination. The population and bond order data calculated for the $Mo_2O_{11}H_{10}$ cluster representing the MoO_3 (010) surface, see Table 1b, are completely analogous to those discussed for V_2O_5 (010) before. The molybdenum centers are described by positive ions $Mo^{+1.3}$ whereas oxygens form negative ions ($O^{-0.4}$ for the terminal and $O^{-0.5}$ for the bridging oxygens). The charge difference between the (more negative) bridging oxygens and the terminal ones is less pronounced for MoO_3 compared to V_2O_5 (010) which is explained by the different coordination geometry of the bridging oxygens. At V_2O_5 (010) oxygens O(b,c) bridge symmetrically between metal ions. In contrast, at MoO_3 (010) the bridging oxygens O(b) form asymmetric bridges, cp. Fig. 1, where O(b) is bound more strongly to the nearer metal center, Mo(2), than to the other, Mo(1), which lies further away. As a result, the binding situation of bridging and terminal oxygens becomes more similar at MoO_3 compared to V_2O_5 (010). This is substantiated by the bond order results given in Table 1b. The O–Mo bonds involving terminal oxygens O(a) are described as O = Mo double bonds (bond order close to 2) analogous to the result for V_2O_5 case. In contrast to V_2O_5, the bond order of bridging oxygens O(b) binding with the Mo(1) centers is only 0.2 suggesting rather weak coupling whereas the value for O(b) binding with the closer Mo(2) is 1.6 indicating a stronger single to double bond. Electrostatic potentials computed from the cluster charge distributions [7] can give additional information about local charging and binding. The spatial variations exhibit negative minima above the open bridging oxygen sites, O(c), on the V_2O_5 (010) surface while on MoO_3 (010) the potential becomes most negative above terminal oxygen O(a) sites. This suggests that positively charged adparticles, like protons resulting from surface reactions, will be attracted at these sites and may form local surface bonds. The difference in the electrostatic potentials between the two substrates is most likely due to structural discrepan-

Table 1

Populations and bond orders obtained from the $V_2O_9H_8$ cluster representing the V_2O_5 (010) surface and of $Mo_2O_{11}H_{10}$ representing MoO_3 (010). The geometric structures of the clusters and the definitions of the different oxygen and metal sites O(a,b,c), V, Mo(1,2) are detailed in Fig. 1. All quantities are given in atomic units

Centers/bonds	Population	Bond order
(a) $V_2O_9H_8$ cluster representing V_2O_5 (010)		
V	22.02	–
O(a)	8.29	–
O(b, c)	8.51	–
O(a)-V	–	2.17
O(b, c)-V	–	0.97
(b) $Mo_2O_{11}H_{10}$ cluster representing MoO_3 (010)		
Mo	40.69	–
O(a)	8.43	–
O(b)	8.54	–
O(a)-Mo	–	1.95
O(b)-Mo(2)	–	1.58
O(b)-Mo(1)	–	0.16

cies which allow for open bridging oxygen sites on V_2O_5 (010) but not on MoO_3 (010).

The left part of Fig. 2 shows results from total energy calculations of hydrogen approaching the V_2O_5 (010) surface simulated by a $(V_2O_9H_8H)^+$ cluster model. Here E_{tot} is displayed as a function of the O–H distance d(O–H) with H adsorbing perpendicular to the surface at the different surface oxygen sites, terminal O(a) and bridging O(b,c), see Fig. 1a. Hydrogen is found to stabilize at all oxygen sites at similar distances d(O–H) (close to the distance of free hydroxyl) where its rather strong binding (resulting in a local OH group) is determined by covalent as well as ionic contributions. The latter is confirmed by the result that the bridging oxygen site O(c) which lead to strongest O–H binding coincides with that where the electrostatic potential of the substrate cluster assumes its (negative) minimum. The right part of Fig. 2 shows total energies of the $(V_2O_9H_8H)^+$ cluster, now better described as $(V_2O_8H_8OH)^+$, where after stabilization of hydrogen the local OH group is removed perpendicular to the surface at the different oxygen sites. Here d(Sub-
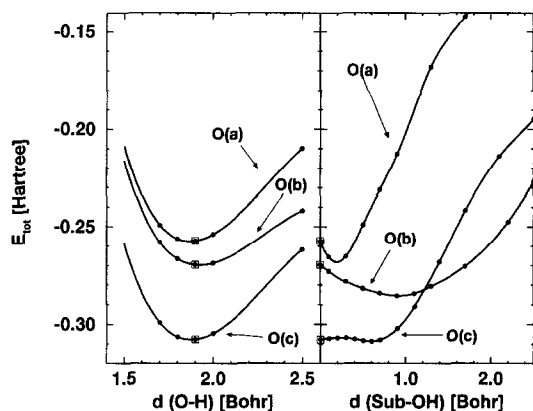

Fig. 3. Potential energy curves for H adsorption and subsequent OH desorption at the MoO_3 (010) surface. The left part shows the total energy of the $(Mo_2O_{11}H_{10}H)^+$ cluster as a function of the O–H distance d(O–H) for H approaching the terminal O(a) and the bridging O(b) sites. The right part gives total energies of $(Mo_2O_{10}H_{10}OH)^+$ where respective OH groups are removed. For a definition of d(Sub-OH) see text.

OH) denotes the OH removal distance with respect to the initial equilibrium geometry of adsorbed hydrogen and d(O–H) is kept fixed in the removal. Obviously, for each oxygen site the minimum energy of the hydrogen binding curve (left figure) coincides with the energy of the OH removal curve at d(Sub-OH) = 0 marked by open squares. For positive distances d(Sub-OH) Fig. 2 reveals a qualitative difference between the different oxygen sites. The removal curve for OH involving a terminal oxygen O(a) exhibits a sharp minimum at d(Sub-OH) = 0.2 Bohr followed by a steep rise which shows that this surface OH group is bound quite strongly to the underlying V metal center. In contrast, the removal curves for OH involving bridging oxygens O(b,c) are rather shallow up to 0.8–1.0 Bohr and the respective surface OH groups can become quite mobile. They are, therefore, much more available for subsequent desorption and reaction than terminal OH groups.

The left part of Fig. 3 shows results for hydrogen approaching the MoO_3 (010) surface simulated by an $(Mo_2O_{11}H_{10}H)^+$ cluster model,

Fig. 2. Potential energy curves for H adsorption and subsequent OH desorption at the V_2O_5 (010) surface. The left part shows the total energy of the $(V_2O_9H_8H)^+$ cluster as a function of the O–H distance d(O–H) for H approaching the terminal O(a) and the two bridging O(b,c) sites. The right part gives total energies of $(V_2O_8H_8OH)^+$ where respective OH groups are removed. For a definition of d(Sub-OH) see text.
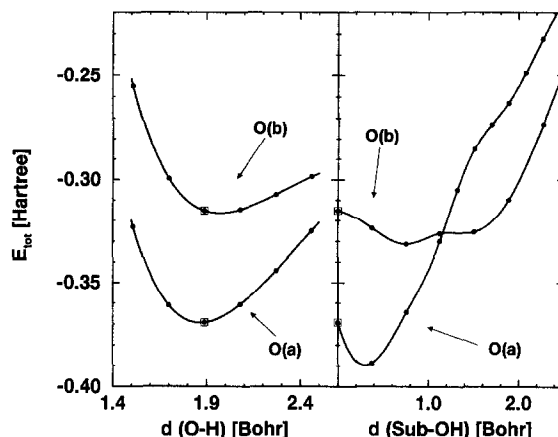
where E_{tot} is given as a function of $d(O–H)$ with H adsorbing at the terminal O(a) and bridging O(b) surface oxygen sites, see Fig. 1b. As for V_2O_5, hydrogen is found to stabilize at both oxygen sites at similar distances $d(O–H)$ forming local OH groups. Here the terminal site O(a) turns out to be energetically most favorable as opposed to the V_2O_5 case where open bridging sites O(c) are preferred. (Symmetric bridging sites O(b') on MoO_3 (010) not considered here are believed to be favored least due to their high metal coordination [7].) This discrepancy can be explained, as for the electrostatic potential results, by structural differences between the two substrates where open bridging oxygen sites O(c) exist on V_2O_5 (010) but not on MoO_3 (010). The participation of ionic contributions to O–H binding at the MoO_3 (010) surface is confirmed by the result that terminal oxygen sites O(a) which lead to strongest binding are the sites where the electrostatic potential of the substrate cluster assumes its (negative) minimum. The right part of Fig. 3 shows total energies of the $(Mo_2O_{11}H_{10}H)^+$ cluster, more appropriately described as $(Mo_2O_{10}H_{10}OH)^+$, where after stabilization of hydrogen the local OH group is removed from different oxygen sites analogous to the above described V_2O_5 case. As before, d(Sub-OH) denotes the OH removal distance with respect to the initial hydrogen equilibrium geometry and $d(O–H)$ is kept fixed in the removal. Fig. 3 shows a removal curve for OH involving the terminal oxygen O(a) which exhibits a sharp minimum at d(Sub-OH) = 0.3 Bohr followed by a steep rise. This proves that the respective surface OH group is bound rather strongly to the underlying Mo metal center. In contrast, the removal curve for OH involving the bridging oxygen O(b) is shallow up to 1.5 Bohr suggesting that respective surface OH groups can become quite mobile. Thus, the qualitative results of Fig. 2 and Fig. 3 concerning OH removal are completely analogous for the two surfaces, V_2O_5 and MoO_3 (010). In both systems OH groups involving terminal oxygens are strongly bound to the sur-

face whereas those involving bridging oxygens are more loosely coupled and can become mobile.

In conclusion, the present cluster calculations on V_2O_5 and MoO_3 (010) reveal pronounced differences between structurally different oxygen sites, terminal oxygens O(a) as well as bridging oxygens O(b,c), at the surfaces. All sites become negatively charged as expected from chemical intuition. Bridging oxygen sites are always found more negative than terminal sites which suggests an increased local reactivity of bridging oxygen sites with respect to nucleophilic attacks [2,16,17]. Binding of hydrogen at the different oxygen sites is determined by covalent as well as ionic contributions leading to local OH surface group formation. While on V_2O_5 (010) the open bridging sites O(c) bind hydrogen most strongly on MoO_3 (010) terminal sites O(a) are energetically preferred. This discrepancy can be explained by structural differences between the two substrate surfaces. Removal of local OH groups after hydrogen adsorption proceeds at both surfaces similarly. OH groups involving terminal oxygens O(a) are quite strongly bound to the surface and are thus unlikely to desorb. In contrast, hydroxyls involving bridging oxygens O(b,c) are more loosely coupled to the surface and mobile about the H adsorption minimum. They are, therefore, available for subsequent reactions and may desorb from the surface. So the present model calculations suggest that bridging oxygen sites, rather than terminal ones, participate in the selective oxidation of hydrocarbons at V_2O_5 and MoO_3(010) surfaces [16,17]. It should be noted that the present model calculations assume a rigid substrate for OH desorption. Thus, possible surface relaxation and reconstruction (requiring multi-dimensional interaction potential evaluations) is neglected and this study accounts only for the initial steps of desorption. However, these initial steps are believed to determine possible reaction channels which will also occur in a full treatment of the surface systems yielding the above conclusions.

References

[1] H.K. Kung, Transition metal oxides: Surface chemistry and catalysis, in B. Delmon and J.T. Yates, Eds., Studies in Surface Science and Catalysis, Vol. 45, Elsevier Science, Amsterdam, 1989.

[2] J. Haber, in J.M. Thomas and K. Zamaraiev, Eds., Perspectives in Catalysis, Blackwell Scientific, Oxford, 1991.

[3] B. Grzybowska-Swierkosz and J. Haber, Eds., Vanadia Catalysts for Processes of Oxidation of Aromatic Hydrocarbons, Polish Scientific, Warsaw, 1984.

[4] E.R. Braithwaite and J. Haber, Eds., Molybdenium: An Outline of its Chemistry and Uses, Studies in Inorganic Chemistry, Vol. 19, Elsevier Science, Amsterdam, 1994.

[5] see e.g. G. Pacchioni, P.S. Bagus and F. Parmigiani, Eds., Cluster Models for Surface and Bulk Phenomena, NATO ASI Series B, Vol. 283, Plenum, New York, 1992.

[6] M. Witko, K. Hermann and R. Tokarz, J. Electr. Spectr. Rel. Phen., 69 (1994) 89.

[7] A. Michalak, M. Witko and K. Hermann, Surf. Sci., submitted.

[8] J.K. Labanowski and J.W. Anzelm, Eds., Density Functional Methods in Chemistry, Springer-Verlag, Berlin, 1991.

[9] N. Godbout, D.R. Salahub, J. Andzelm and E. Wimmer, Can. J. Phys., 70 (1992) 560.

[10] J. Andzelm, E. Radzio and D.R. Salahub, J. Chem. Phys., 83 (1985) 4573.

[11] The LCGTO-LSD-DFT program package DeMon was developed by A. St-Amant and D. Salahub at the University of Montreal.

[12] S.H. Vosko, L. Wilk and M. Nusair, Can. J. Phys., 58 (1980) 1200.

[13] R.S. Mulliken, J. Chem. Phys., 23 (1955) 1833, 1841, 2388, 2343.

[14] I. Mayer, Chem. Phys. Lett., 97 (1983) 270.

[15] R. Bonaccorsi, E. Scrocco and J. Tomasi, J. Chem. Phys., 52 (1970) 5270.

[16] M. Witko, J. Mol. Catal., 70 (1991) 277.

[17] M. Witko and K. Hermann, J. Mol. Catal., 81 (1993) 279.